

Winter Monthly Mean Atmospheric Anomalies over the North Pacific and North America Associated with El Niño SSTs

HUI WANG* AND RONG FU*

Institute of Atmospheric Physics, University of Arizona, Tucson, Arizona

(Manuscript received 22 January 1999, in final form 11 January 2000)

ABSTRACT

The characteristics of winter monthly mean extratropical circulation associated with El Niño, including precipitation and surface temperature over the United States, are examined for nine El Niño events during 1950–94. Precipitation and surface temperature over the United States, also the 500-mb geopotential height and sea level pressure over the North Pacific and North America, are significantly different between early winter (November and December) and late winter (January to March). The typical El Niño-related U.S. precipitation and surface temperatures identified in many previous studies, as well as the Pacific–North American (PNA) circulation pattern, emerge in January and persist through February and March. The PNA patterns during these late winter months are coupled both with the tropical El Niño sea surface temperature (SST) variation and with the North Pacific SST variation. In contrast, the PNA patterns in the early winter months correlate only with the North Pacific SST. The tendency for the PNA pattern to occur during El Niño years is much less in early winter months than in late winter months. An ensemble analysis of 12 45-yr (1950–94) integrations of the National Center for Atmospheric Research Community Climate Model forced by the observed time-varying SST shows that the model 500-mb heights display a PNA-like pattern in both early and late winters of El Niño. The ensemble model response to the El Niño SST is thus unable to reproduce the observed differences in the extratropical atmospheric circulation between early and late winter months.

1. Introduction

Substantial progress has been made during the past two decades toward understanding the wintertime extratropical atmospheric response to the tropical forcing associated with El Niño sea surface temperature (SST) anomalies (Trenberth et al. 1998). Both observational and theoretical studies demonstrate that Rossby wave dynamics link the changes in the extratropical circulation to the tropical SST (e.g., Wallace and Gutzler 1981; Horel and Wallace 1981; Hoskins et al. 1977; Hoskins and Karoly 1981). Associated with the tropical El Niño SST, the most prominent teleconnection pattern is the Pacific–North American (PNA) pattern (Horel and Wallace 1981). This pattern is very reproducible in atmospheric general circulation models (AGCMs) when El Niño–like SSTs are prescribed in the tropical Pacific (e.g., Blackmon et al. 1983; Lau 1985).

In addition to the fundamental Rossby wave propagation from the tropical heating source, there are other basic mechanisms that are important in determining the extratropical atmospheric response to a tropical forcing. As reviewed by Trenberth et al. (1998), these mechanisms include the normal-mode instability of zonally varying climatological mean flow (Simmons et al. 1983) and the influence of midlatitude transient eddies associated with storm tracks (Kok and Opsteegh 1985; Held et al. 1989; Hoerling and Ting 1994). The two mechanisms are shown to be more effective than the tropical El Niño SST in governing the structure and geographic locations of the PNA pattern. These studies focused on identifying the energy sources of the wintertime teleconnection pattern. Given the fact that anomalous warm tropical SSTs during El Niño exist prior to winter, little is known about the timing of the PNA pattern associated with the tropical SST.

An observational study by Wallace and Jiang (1987) demonstrates that the atmospheric PNA pattern correlates more closely with the North Pacific SST anomalies than it does with the tropical SST. Several modeling studies, including Alexander (1990, 1992) and Lau and Nath (1996), suggest that the observed North Pacific SST anomalies during El Niño are primarily due to the oceanic response to atmospheric circulation forced by the tropical SST. Using an AGCM coupled with an

* Current affiliation: Georgia Institute of Technology, Atlanta, Georgia.

Corresponding author address: Hui Wang, School of Earth and Atmospheric Sciences, Georgia Institute of Technology, 221 Bobby Dodd Way, Atlanta, GA 30332-0340.
E-mail: huiwang@eas.gatech.edu

ocean mixed layer model, Lau and Nath (1996) further illustrated that the extratropical air–sea interaction reinforces the atmospheric anomalies in the PNA pattern. This suggests that the North Pacific SST might be involved in the extratropical atmospheric response to the tropical forcing.

The extratropical atmospheric response to the tropical El Niño SST strongly influences U.S. precipitation and surface air temperatures in the winter season, as documented in many studies (e.g., Ropelewski and Halpert 1986, 1987; Halpert and Ropelewski 1992; Wang 1997). In these studies, the winter season generally refers to the months of December–February, and sometimes November–March. Averaged over November–March, both U.S. precipitation and temperature respond to El Niño in a way consistent with the PNA pattern, namely: wetter conditions over the Gulf Coast states, southern plains, southern Northwest, and California; drier conditions over the Ohio River valley and northward to the east of the Great Lakes; and warmer temperatures over most of the United States, except for the Southeast where temperatures are below normal. On a *monthly* timescale, however, precipitation and temperature anomalies may deviate from the typical El Niño–related seasonal means. During the 1982/83 El Niño, for example, large positive rainfall anomalies extended all the way from the Gulf states to the Great Lakes in December. In the same month, cold temperature anomalies covered California, southern Arizona, New Mexico, and Texas, rather than the Southeast, and warm anomalies dominated the east of the country. The significant differences in monthly precipitation anomalies over the central and eastern United States between early (November and December) and late winters (January–March) of El Niño are also identified in Montroy (1997) and Montroy et al. (1998).

Livezey et al. (1997) conducted a series of composites on monthly mean U.S. precipitation and surface temperature and 700-mb height based on warm SST anomalies in the tropical Pacific. Their analysis reveals the distinctions in U.S. precipitation anomalies between early and later winters of El Niño. They also found that associated with El Niño, there are no significant 700-mb height signals in early winter months, but well-defined PNA patterns in later winter. The PNA pattern is one of the most frequently occurring extratropical circulations throughout the winter months (Barnston and Livezey 1987), and is highly correlated with the North Pacific SST (Wallace and Jiang 1987). The evidence naturally poses one question, that is, what SST patterns tend to occur simultaneously with the prominent extratropical circulation anomalies.

This study is aimed at examining the characteristics of El Niño–related monthly mean U.S. precipitation and surface air temperature, as well as the PNA pattern and its relation to both tropical and North Pacific SST anomalies. In particular, the present work complements the contribution of Livezey et al. (1997) et al. by consid-

ering midlatitude SST patterns that tend to accompany the prominent atmospheric anomalies. In the next section, the data and statistical methods are described. Section 3 describes monthly (November–March) U.S. precipitation and temperature anomalies and corresponding atmospheric circulation patterns during El Niño. The covariability between extratropical circulation and Pacific SST is examined in section 4. Section 5 analyzes an ensemble atmospheric response to the Pacific SST from 12 45-yr (1950–94) integrations of the National Center for Atmospheric Research (NCAR) Community Climate Model (CCM3), forced by the observed time-varying SST, and compares the model results to the observations. Conclusions are given in section 6.

2. Data and methods

The observational data used in this study consist of monthly mean U.S. precipitation and temperature, Pacific SST, Northern Hemisphere 500-mb geopotential height, and sea level pressure (SLP) from 1950 to 1994. An anomaly is defined as the deviation of monthly mean from its climatological mean value. The precipitation data are from the Global Historical Climatology Network for 1950–90 (Vose et al. 1992) and from the Gridded Hourly Precipitation Data Base for the United States for 1991–94 (Higgins et al. 1996), and are processed into a $2.5^\circ \times 2.5^\circ$ latitude–longitude grid. The surface air temperatures are from the Climate Anomaly Monitoring System developed at the National Centers for Environmental Prediction (NCEP) on a $2^\circ \times 2^\circ$ grid. The SSTs are from the NCEP-reconstructed SST dataset (Smith et al. 1996) on a $2^\circ \times 2^\circ$ grid. The 500-mb height and SLP are from the NCEP operational analyses. The data are analyzed on a 2.5° latitude by 5° longitude grid over the Northern Hemisphere from 20° to 90°N . A more detailed description of the data and their quality can be found in Ting and Wang (1997).

Composite and singular value decomposition (SVD) (Bretherton et al. 1992; Wallace et al. 1992) analyses are applied to the atmospheric circulation for nine El Niño winters during 1950–94 and to the 45-yr 500-mb height and Pacific SST, respectively. The composite provides amplitudes of atmospheric anomalies associated with El Niño. The El Niño years are chosen based on a definition of El Niño in Trenberth (1997) that 5-month running mean SST anomalies in the Niño-3.4 region (5°S – 5°N , 120° – 170°W) are greater than 0.4°C and last for 6 months or more. The nine events are the winters of 1957/58, 1965/66, 1968/69, 1969/70, 1972/73, 1982/83, 1986/87, 1987/88 and 1991/92. The SVD objectively identifies pairs of spatial patterns with maximum temporal covariance between the atmospheric circulation and the SST.

The statistical significance of both composite anomalies and correlations is estimated by the Monte Carlo technique. The basic idea is to construct many new time series with the same size as the original one by resam-

pling the temporal points at random order from the original data. The composites and correlations using these new data produce a pool of reference test statistics. If a value calculated using the original data is high enough to fall into the top 5% rank in the reference test statistics, then it is defined to exceed the 95% significance level.

3. Monthly mean U.S. precipitation, surface temperature, and circulation anomalies during El Niño

a. Composites of precipitation and surface temperature

Figure 1 presents the composite of monthly mean U.S. precipitation anomalies for the nine El Niño winters. In November and December (Figs. 1a and 1b), wetter conditions dominate the eastern, central, and southwestern United States. The largest positive rainfall anomalies are found in the lower Mississippi River basin. In January through March (Figs. 1c–e), precipitation is below normal in the Ohio River valley and above normal in the Gulf Coast and some parts of the southern plains and the Southwest. Figure 1 indicates that precipitation in late winter is similar to the typical El Niño–related seasonal mean pattern, as identified in many previous studies (e.g., Ropelewski and Halpert 1986, 1987; Wang 1997), while precipitation in early winter is not.

The composite of surface air temperature anomalies is shown in Fig. 2. In November, temperature is below normal over most of the nation though insignificant. In contrast, warm temperature anomalies are found everywhere in December, except California. In January–March, temperature anomalies show a dipole structure, with warmer temperatures in the north and colder temperatures to the south. The pattern resembles the El Niño–related seasonal mean (Ropelewski and Halpert 1986).

Both U.S. precipitation and temperature anomalies during El Niño show apparent differences between early and late winters, especially between December and January–March. Similar differences are found in the composites by Livezey et al. (1997) and Montroy et al. (1998), though the El Niño years chosen in their analyses are slightly different from those in this study. The composite signals in Figs. 1 and 2 are statistically significant. They suggest that different processes may be responsible for the anomalous patterns in the early and late winters.

b. Composites of 500-mb height and SLP

To ascertain the physical processes responsible for the differences in U.S. precipitation and temperature between early and late El Niño winters, the composites of monthly mean 500-mb height anomalies for the nine El Niño years are shown in Fig. 3. The circulation illustrates clearly different patterns between early and late

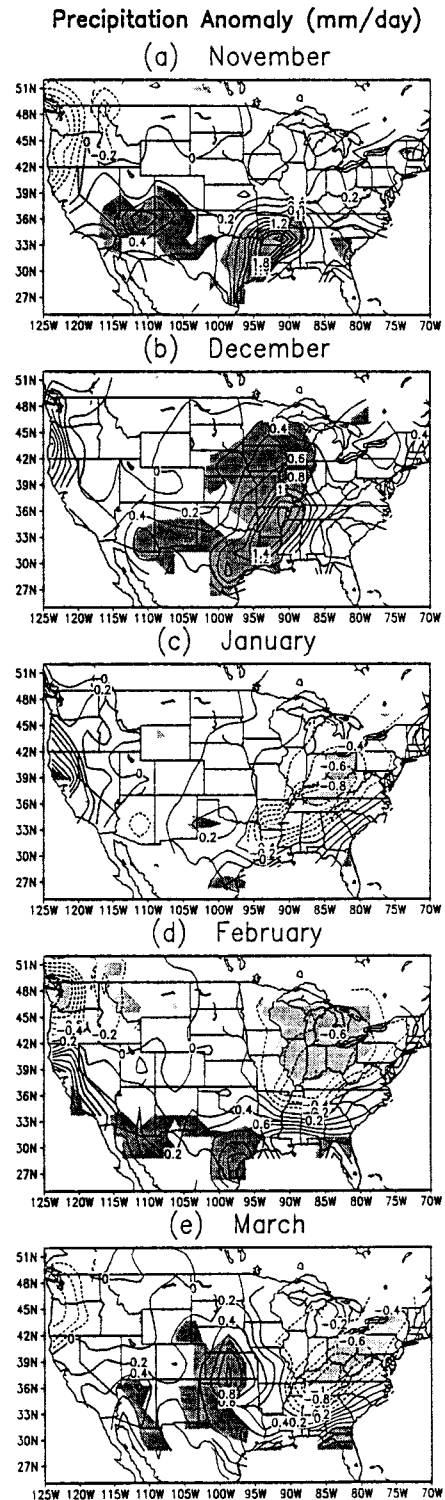


FIG. 1. Composite of monthly mean U.S. precipitation anomalies for the nine El Niño winters. The contour interval is 0.2 mm day^{-1} , and negative values are dashed. Dark (light) shading indicates the statistical significance of positive (negative) values at the 95% confidence level using Monte Carlo test.

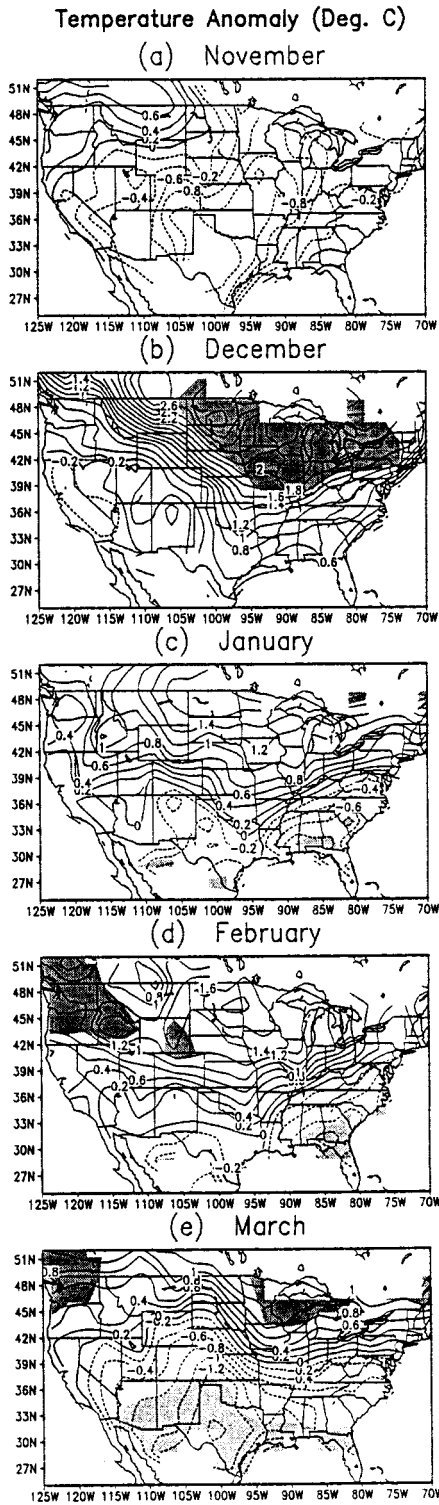


FIG. 2. Composite of monthly mean U.S. surface air temperature anomalies for the nine El Niño winters. The contour interval is 0.2°C, and negative values are dashed. Shadings are the same as in Fig. 1.

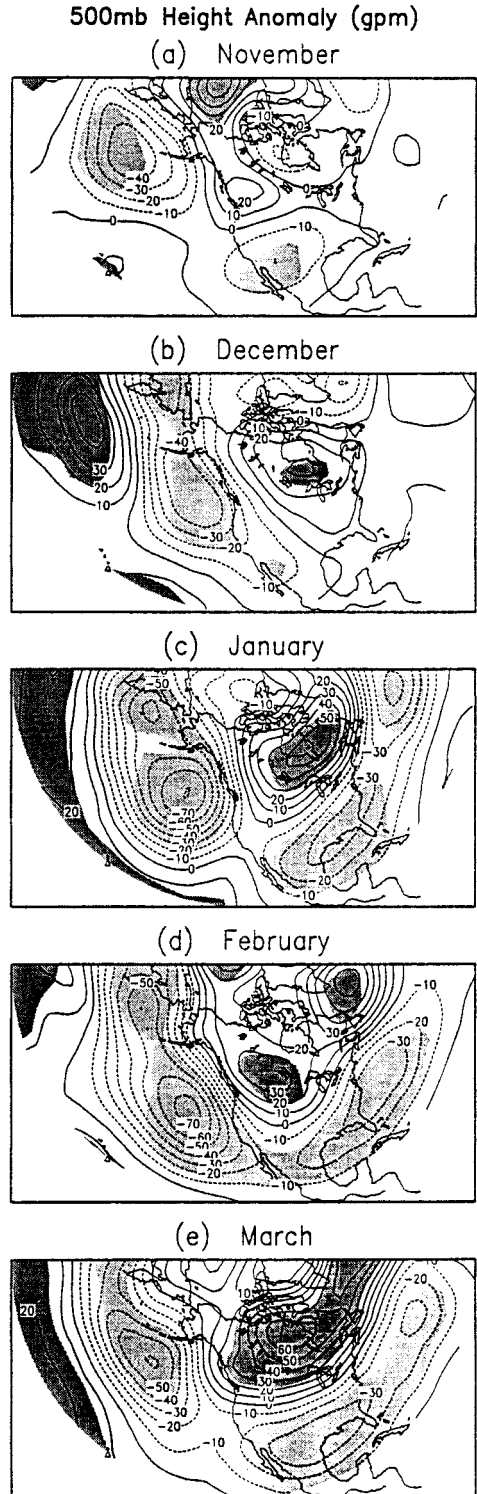


FIG. 3. Composite of monthly mean 500-mb height anomalies for the nine El Niño winters. The contour interval is 10 gpm, and negative values are dashed. Shadings are the same as in Fig. 1.

winter months, consistent with those of U.S. precipitation. In November there is a center of negative height anomalies over the central North Pacific. The height anomalies are weak over North America. The December circulation pattern shifts toward the east relative to November. There are significant positive anomalies over the central North Pacific and Canada, and negative anomalies along the West Coast, indicating a teleconnection pattern. In January both negative and positive anomalies over the eastern North Pacific and Canada are intensified. In the meantime, large negative height anomalies emerge and dominate over the southern states, Gulf of Mexico, and North Atlantic. The PNA pattern is clearly identified in January and persists through February and March. Associated with these circulation anomalies, there are southerly winds over the southern plains and the Southeast in November and December. The circulation thus favors low-level moisture transport inland and enhances rainfall in these regions (Figs. 1a and 1b). In January–March there are westerly anomalies in the Gulf of Mexico and northern Mexico, and easterly to the north in company with the negative height anomalies. Consequently, the upper-level jets shift to the south.

The SLP anomalies in each month (Fig. 4) display a spatial pattern similar to the corresponding 500-mb height. The isobars over the United States are largely zonal in November but become meridional in December. Since winter mean temperature is dominated by a strong meridional gradient with warm (cold) temperature in the south (north), anomalous southerly surface winds are generally associated with warm advection. This may account for the differences in temperature anomalies between November and December (Fig. 2). In January–March, a PNA-like pattern can be seen in the SLP field. The temperature anomalies in these months (Fig. 2) are consistent with the thermal advection associated with the SLP patterns.

The composites of both upper- and low-level circulation reveal distinctions between early and late winters of El Niño. A PNA pattern is well established in January and persists in the following two months. The circulation patterns are consistent with the monthly mean precipitation and temperature anomalies over the United States. The results illustrate the timing of the extratropical circulation during El Niño winters.

4. Relationships of the extratropical circulation to Pacific SSTs

a. Results from the SVD analysis

The composite analysis suggests a coupling between the PNA pattern and El Niño. The strength of the coupling can be quantitatively examined using the SVD method, based on the cross-covariance matrices of monthly mean 500-mb height (20° – 90° N, 150° E– 30° W) and Pacific SST (20° S– 60° N, 120° E– 80° W). The first

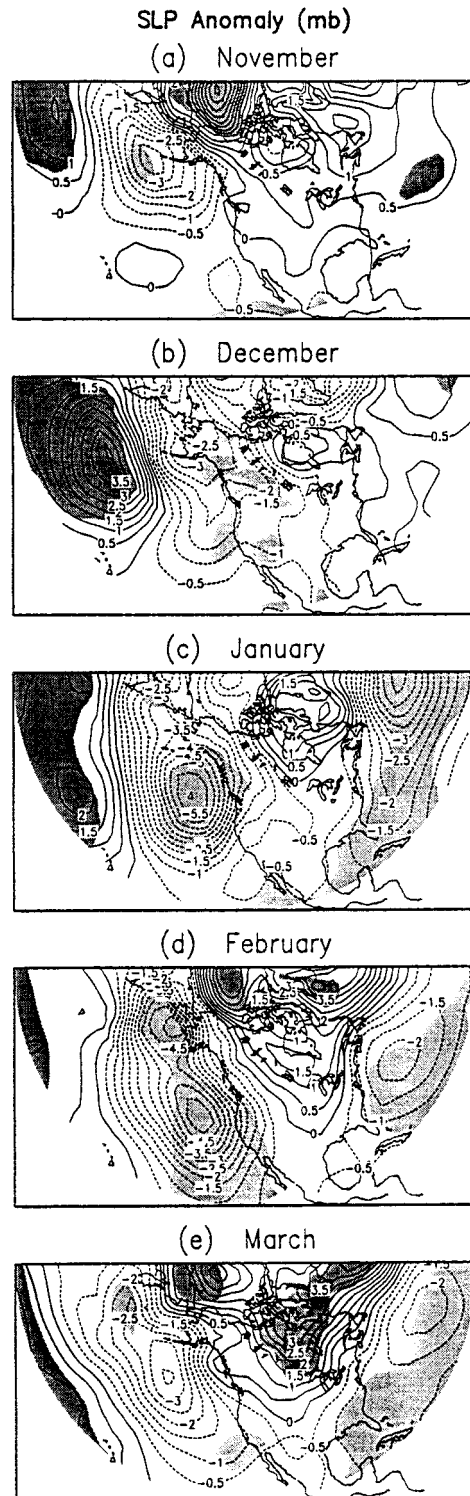


FIG. 4. Composite of monthly mean sea level pressure anomalies for the nine El Niño winters. The contour interval is 0.5 mb, and negative values are dashed. Shadings are the same as in Fig. 1.

SVD mode in each winter month, except for November, captures the El Niño SST variability coupled with the 500-mb height. The homogeneous correlation maps (Wallace et al. 1992) for the SST, which are the spatial patterns of the SST projected onto the SVD SST eigenvectors, display a typical El Niño SST pattern (not shown). The largest positive correlations are found in the eastern and central equatorial Pacific, with negative correlations in the central North Pacific and positive correlations along the North American coast. The month-to-month autocorrelations of the SST time series of the first SVD modes all exceed 0.9, indicating a strong persistence of the El Niño SST throughout the cold season.

The SST anomalies that are actually related to the 500-mb heights in the first SVD modes can be seen in heterogeneous correlation maps (Wallace et al. 1992), which are the correlations of SST anomalies (Fig. 5, left) with the time series of the 500-mb height SVD modes. In November the first SVD mode shows that only the North Pacific SST anomalies are relevant. The 500-mb height (Fig. 5, right) displays a wave structure, but different from the PNA pattern. In December both tropical and North Pacific SSTs are involved. The SST displays an El Niño-like pattern. In January–March the SST patterns consist of large negative correlations in the central North Pacific along 30°N and positive correlations in the eastern North Pacific and in the Tropics. The PNA patterns are found only in January–March and correlate more closely with the North Pacific SST than the tropical SST. The first SVD modes indicate that the SST anomalies of different regions dominate the coupling with the extratropical circulation in different months. The occurrence of the PNA pattern is strongly related to the North Pacific SST.

The homogeneous correlations of the November SST in the second SVD mode also display an El Niño-like pattern (not shown). The heterogeneous correlations (Fig. 6a) indicate that only the eastern tropical Pacific SST anomalies are involved in coupling with the extratropical circulation. The SVD analysis thus effectively separates the relation of the November 500-mb circulation to the tropical SST from its relation to the North Pacific SST. The circulation associated with the North Pacific SST (mode 1) is stronger than that associated with the tropical SST (mode 2).

The strength of the coupling between Pacific SST and extratropical atmospheric circulation and their contribution to the total variability are examined using some SVD statistics. Table 1 lists the squared covariance fraction (CVR) explained by each SVD mode, the temporal correlation (r) between each pair of SVD time series, and the percentage of variance (VR) in individual fields explained by their corresponding component in each SVD mode. The values in parentheses are the percentages when only the nine El Niño years are taken into account. In November the first SVD mode explains 56% of the total squared covariance (CVR) between SST and

500-mb height, much higher than the El Niño-related second mode (21%). The first mode explains 36% of the variance (VR) in the 500-mb height for the whole period, but only 6% for the nine El Niño years. This indicates a strong link between the North Pacific SST and atmospheric circulation in November, and little contribution from the tropical El Niño SST. The strongest coupling between 500-mb height and El Niño SST occurs in January–March with the total squared covariance (CVR) exceeding 50% and temporal correlation coefficients (r) greater than 0.60. In general, the warm tropical SST anomalies during El Niño reach their maximums in December or January, then decrease in the following months. This is consistent with the largest percentages of the SST variance (VR) explained by the SVD modes in these two months, especially for the nine El Niño years. The percentages of the 500-mb height variance, however, are relatively small in December and January, but increase in late winter after the maturity of the El Niño SST. Moreover, the increases in the percentages of variance in the 500-mb height, when considering only the nine El Niño years, are not as large as those for the SST. The results suggest that the El Niño SST influence on the extratropical circulation is limited. Other processes, such as atmospheric internal variability and extratropical air–sea interaction, may also contribute to the variation of the PNA pattern.

b. Associations between the PNA pattern and El Niño in early and late winter

Zhang et al. (1996) demonstrated that the PNA pattern in 500-mb height is coupled with the North Pacific SST when the variability linearly associated with El Niño is removed from the height field. In this section, we examine the relationships between the PNA pattern and El Niño in early and late winter months. We performed an empirical orthogonal function (EOF) analysis on the monthly mean 500-mb height over the PNA regions. The PNA pattern (not shown) is well selected by the first EOF modes in November–February and by the second mode in March. If we define the EOF expansion coefficients exceeding 0.5 standard deviation as an occurrence of the PNA pattern, then Table 2 presents the numbers of months with PNA patterns in the 45 years (1950–94) and in the nine El Niño years, respectively. The frequency of occurrence of the PNA pattern is much lower during non-El Niño years than during El Niño years. The total number of the months with the PNA pattern during the 45-yr period, as well as the percentage of the variance explained by the PNA-like EOF mode, does not vary too much from November to March. However, less PNA patterns are found in November and December of the El Niño years (<30%), and more are found in January–March (>40%). This is consistent with the composite and SVD analyses, in which the PNA patterns coupled with the El Niño SST are found only in January–March. The number of months in Table 2 is

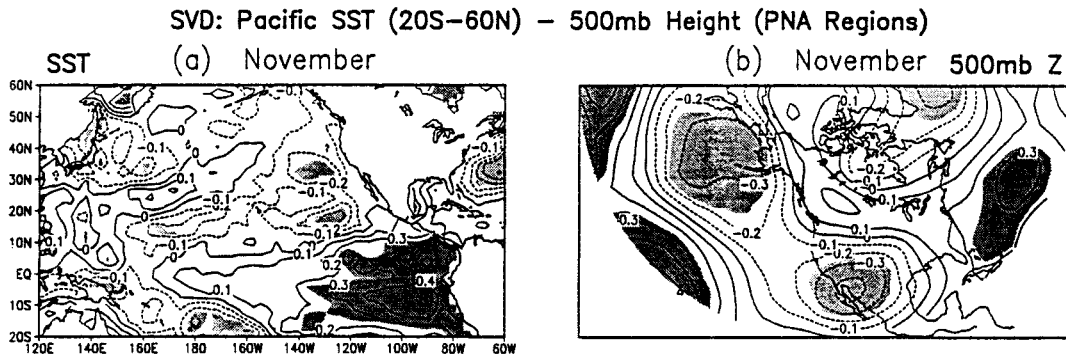


FIG. 6. Same as Fig. 5, but for the second SVD mode of Nov SST and 500-mb height.

sensitive to the criterion we define for the occurrence of the PNA pattern, but the tendency in the percentage of occurrence in the El Niño years is not.

The relationship between the PNA pattern and Pacific SST can also be examined in the correlations of SST with the expansion coefficients of the PNA-like EOF modes, as shown in Fig. 7. In November and December the PNA patterns significantly correlate with the North Pacific SST. There are also positive correlations with the tropical SST centered between 10° and 20°S in the eastern Pacific in November and in the western tropical Pacific in December. The correlations with the eastern and central tropical Pacific SSTs are relatively weak in December. The correlation patterns of SST in January–March are very similar to the heterogeneous one (Fig. 5). The correlation coefficients are significant in both the Tropics and extratropics, but stronger in the extratropics. Figure 7 reveals that both tropical and North Pacific SSTs are strongly related to the PNA pattern in all five months, but with distinctions in the Tropics between early winter and late winter. This confirms the results in the SVD analysis.

5. Atmospheric response to Pacific SST in the NCAR CCM3

The above observational analyses are limited in their ability to separate atmospheric external variability driven by the SST from the internal. This shortcoming can be partially overcome by analyzing ensemble results of

AGCM simulations with appropriate SST prescribed as a boundary condition. The atmospheric responses to the observed global SST from 1950 to 1994 in the NCAR CCM3 are adopted for our purpose. A detailed description of the CCM3 was given in Kiehl et al. (1998). The NCEP reconstructed SST used in the above analyses was prescribed as a boundary forcing to drive the model (Saravanan 1998). Twelve parallel integrations subjected to identical time-varying SSTs have been performed by the Atmosphere Model Working Group at NCAR. Each realization starts from a different initial condition. Our analyses focus on the ensemble averages of 500-mb heights in the 12 simulations. The results will provide a clear indication of the atmospheric response to SST forcing.

a. 500-mb height composites

Figure 8 shows the composite of monthly mean 500-mb height anomalies in CCM3 for the nine El Niño winters. Despite some minor differences in the locations of maximum anomalies, the model response to El Niño SST displays a PNA-like pattern in all five months. The pattern correlations between the height anomalies in observations (Fig. 3) and in CCM3 (Fig. 8) are 0.65, 0.74, 0.68, 0.49, and 0.76, respectively, from November to March. In early winter the model circulation patterns disagree with observations in North America (Figs. 3a and 3b). The pattern correlation is relatively low in November (0.65). A high pattern correlation in November (0.74) is due to the coincidence of centers of anomalies in the North Pacific and Canada between observations

TABLE 1. Summary of the statistics of the first SVD modes between the 500-mb height and Pacific SST, including Mode 2 in Nov. The percentages in parentheses are those when only the nine El Niño years are taken into account.

Month	CVR	<i>r</i>	SST VR	500-mb height VR
Nov (Mode 1)	56%	0.46	19% (20%)	36% (6%)
Nov (Mode 2)	21%	0.40	25% (39%)	13% (12%)
Dec (Mode 1)	45%	0.53	45% (61%)	9% (12%)
Jan (Mode 1)	58%	0.64	39% (51%)	15% (18%)
Feb (Mode 1)	65%	0.62	28% (32%)	28% (29%)
Mar (Mode 1)	52%	0.62	30% (44%)	18% (21%)

TABLE 2. Number of months with the PNA pattern.

Percentage of variance	45 yr (1950–94)	9 El Niño yr	Percentage of occurrence in the 9 El Niño yr
Nov 23% (Mode 1)	18	5	27%
Dec 24% (Mode 1)	14	2	14%
Jan 28% (Mode 1)	14	6	43%
Feb 29% (Mode 1)	14	6	43%
Mar 21% (Mode 2)	15	6	40%

Corr(SST, 500mb Height PNA-Like EOF Mode)

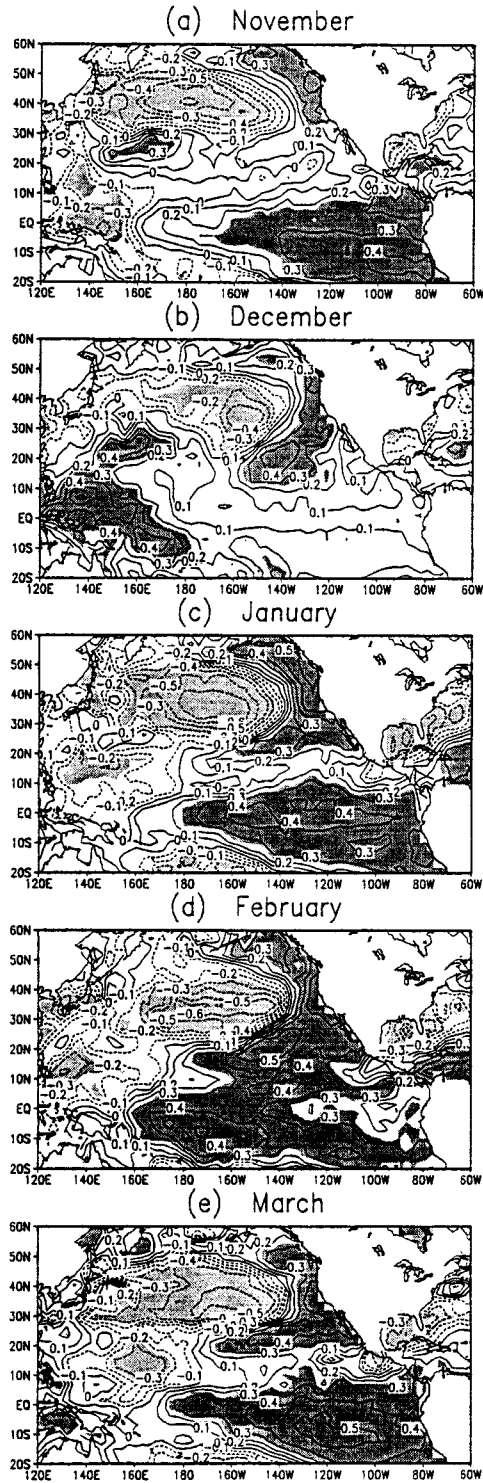


FIG. 7. Correlation patterns of the SST with the expansion coefficients of the PNA-like EOF mode of the monthly mean 500-mb height. Contours and shadings are the same as in Fig. 5.

500mb Height Anomaly (gpm) CCM3

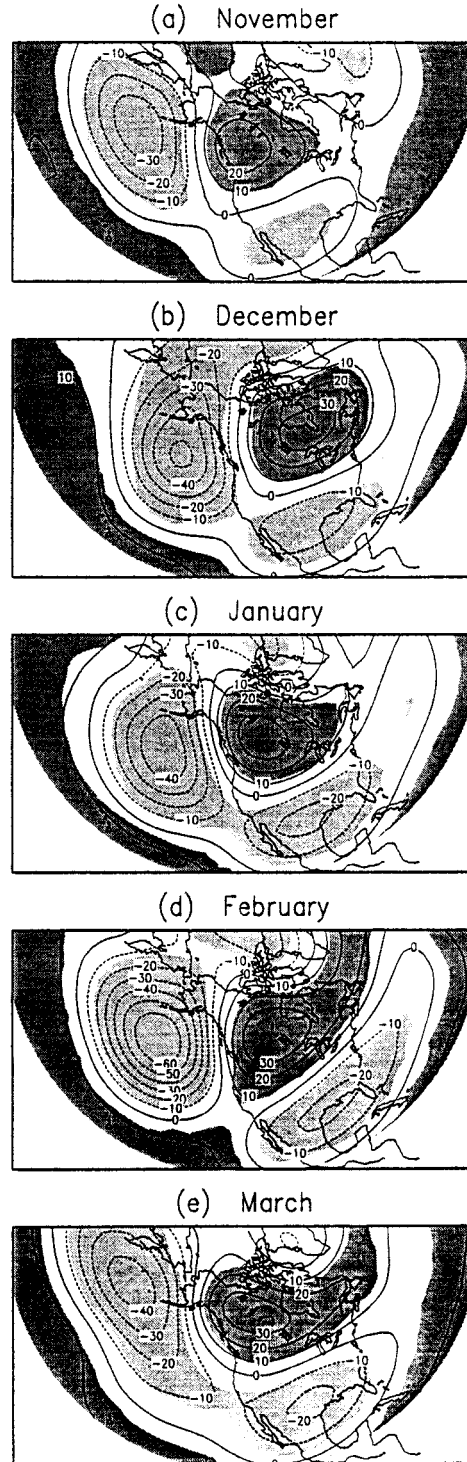


FIG. 8. Composite of monthly mean 500-mb height anomalies in the model simulations for the nine El Niño winters. The contour interval is 10 gpm, and negative values are dashed. Shadings are the same as in Fig. 1.

and the model. In late winter (January–March) the model circulation is weaker than that in observations (Figs. 3c–e), but their patterns are similar to each other. In February the shift of two centers of negative height anomalies in CCM3 relative to observations leads to the lowest pattern correlation (0.49) among the five months. In January and March the pattern correlations (0.68 and 0.76) are highly significant. The result indicates that the ensemble model circulation does not adequately capture the observed timing of the extratropical circulation patterns during El Niño. A similar problem also exists in the ensemble analysis of the NCEP Medium-Range Forecast Model (see Fig. 18 in Livezey et al. 1997).

b. Extratropical circulation variability forced by the Pacific SST

To quantify the SST-forced extratropical circulation variability in the model, an SVD analysis is performed on the observed monthly mean Pacific SST and the model 500-mb height over the PNA regions. The heterogeneous correlation patterns of the first SVD mode for SST display an El Niño SST distribution in all five months (Fig. 9, left), suggesting that El Niño dominates the variability of the SST forcing in the model. Unlike observations (Fig. 5, left), the correlations of SST (Fig. 9) are stronger in the Tropics than in the North Pacific. A close inspection reveals some differences in SST between early and late winter months. Both centers of positive correlations in the tropical Pacific and negative correlations in the central North Pacific are located farther westward in November than in any other months. In particular, there are positive correlations in the eastern North Pacific around 50°N in November.

The heterogeneous correlation pattern of the November 500-mb height in Fig. 9 (top right) resembles to some extent both the first and second SVD modes in observations (Figs. 5 and 6) that are coupled with the North Pacific SST and eastern tropical Pacific SST, respectively. Since strong SST signals are found in both the Tropics and extratropics (Fig. 9, top left), the first SVD mode of the November circulation in the model captures the extratropical circulation associated with both tropical and North Pacific SSTs. From December to March, the 500-mb height circulation in the first mode (Fig. 9, right) displays very similar structures, that is, the PNA pattern. The centers of action in these months shift slightly toward the east relative to November. This may be a response to the shift of the SST patterns between November and the following months (Fig. 9, left). Among the five winter months, the largest disagreement between the model circulation and observations (Figs. 5 and 9) is found in December. The December circulation in the model is more closely correlated with the North Pacific SST than it is in observations. Consistent with the composite analysis, the SVD analysis on the ensemble model response does not distinguish the dif-

ferences between early and late winter circulation associated with El Niño either.

Parallel to Table 1, Table 3 examines the strength of coupling between Pacific SST and model 500-mb height in the first SVD mode and their contribution to the total variance simulated by the CCM3. Those in parentheses are the corresponding values when only the nine El Niño years are taken into account. Both the percentages of covariance ($>75\%$) and the temporal correlations (>0.75) between SST and 500-mb height indicate that the model circulation is dominated by the response to the El Niño SST variation throughout the winter months. In particular, the percentages of the 500-mb height variance during El Niño years are between 40% and 70%. The El Niño SST is thus responsible for a large amount of forced circulation variability.

c. Relationship between occurrence of the PNA pattern in CCM3 and El Niño

Similar to the observational analysis, the frequency of occurrence of the PNA pattern in CCM3 during El Niño is also examined. We conducted the EOF analysis on the ensemble model 500-mb heights. The PNA pattern is picked out by the first EOF mode in each month. Table 4 shows the numbers of months with the PNA pattern, using the criterion of the relevant EOF expansion coefficients greater than 0.5 standard deviation for an occurrence of the PNA pattern. The ensemble-averaged model circulation has higher percentages of occurrence of the PNA pattern during El Niño than the observed circulation in all five months. Since an ensemble average reduces the internal variability of the atmosphere, the above result is biased toward the external response. To compensate for this, the EOF method is applied to individual CCM3 runs. The numbers of months with the PNA pattern averaged from 12 CCM3 runs are also listed in Table 4 (in parentheses). On average, the numbers of months with the PNA pattern in individual runs are greater than the ensemble means for the 45-yr period, except for February, but they are smaller than the ensemble averages for the nine El Niño years. This indicates that the internal variability tends to reduce the percentages of occurrence of the PNA pattern in El Niño years. A comparison between the percentages in Tables 2 and 4 may suggest that the El Niño SST is more responsible for the PNA patterns in later winter than it is in early winter.

6. Conclusions

Using monthly mean data, we showed that the U.S. precipitation and temperature anomalies in the early winters of El Niño are significantly different from the well-identified, El Niño-related seasonal means. Differences also exist in the 500-mb height and SLP between early (November and December) and later winters (January–March), consistent with those in U.S. precip-

SVD: Pacific SST (20S–60N) – 500mb Height (PNA Regions) CCM3

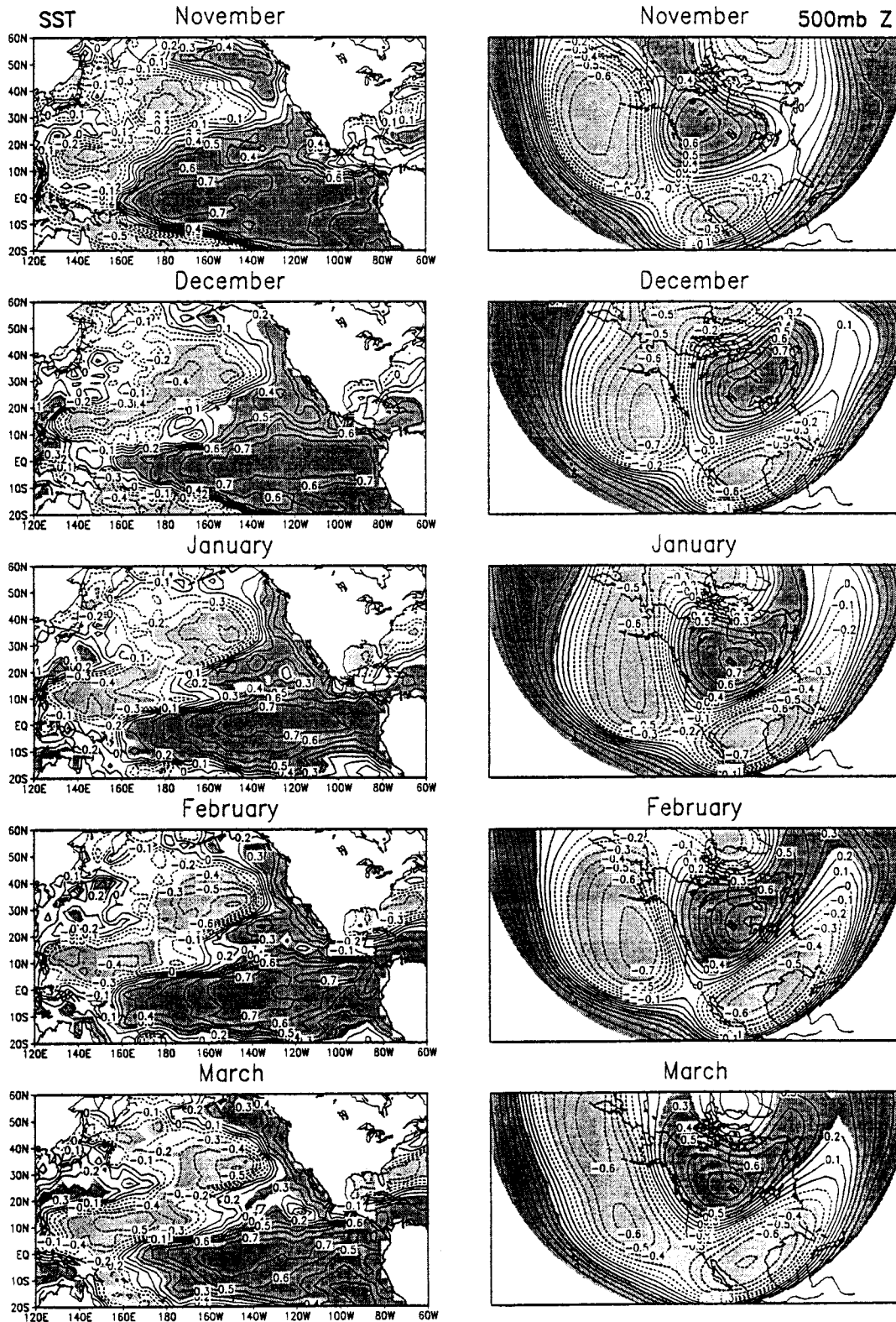


FIG. 9. Heterogeneous correlation patterns of SST (left) and model 500-mb height (right) of the El Niño-related SVD modes for Nov–Mar. The contour interval is 0.1, and negative values are dashed. Shadings are the same as in Fig. 1.

TABLE 3. Summary of the statistics of the first SVD modes between the 500-mb height in CCM3 and Pacific SST. The percentages in parentheses are those when only the nine El Niño years are taken into account.

Month	CVR	r	SST VR	500-mb height VR
Nov (Mode 1)	92%	0.76	45% (60%)	35% (43%)
Dec (Mode 1)	92%	0.79	46% (66%)	38% (66%)
Jan (Mode 1)	87%	0.75	44% (62%)	35% (47%)
Feb (Mode 1)	84%	0.78	37% (56%)	37% (69%)
Mar (Mode 1)	78%	0.76	34% (53%)	33% (55%)

itation and temperatures. The PNA circulation pattern, associated with El Niño, is not completely established until January, suggesting the timing of the extratropical response to tropical forcing. Thus, from a statistical perspective, it would be more consistent to consider January–March as a winter season, in terms of the El Niño influence on extratropical circulation.

The different characteristics of the PNA pattern between early winter and late winter documented in this study are consistent with some previous studies. Using monthly mean 700-mb heights over the Northern Hemisphere, Barnston and Livezey (1987) found that the PNA pattern is selected by one of the two leading EOF modes in January and February but by the sixth EOF mode in December. Livezey and Mo (1987) illustrated that the extratropical responses to the El Niño-related tropical heating, including the PNA pattern, are stronger in January and February but weaker in December. Recently, Newman and Sardeshmukh (1998) examined the impact of the annual cycle of the background flow on the linear extratropical response to tropical forcing. They suggested that it is not always appropriate to use seasonal mean data in the study of the low-frequency circulation. The dependence of the extratropical atmospheric response on the climatological mean flow may be one of the reasons for the differences in the PNA pattern between early winter and later winter. One aspect of this study, which is new relative to the previous work, is that the occurrences of a PNA pattern in early winter are primarily associated with the North Pacific SST, while in later winter they are associated with both the El Niño-related tropical SST and the North Pacific SST. The results indicate a seasonality of Pacific SST in company with the prominent atmospheric circulation anomalies.

The atmospheric circulation associated with the variability of Pacific SST was also assessed by analyzing the 12 NCAR CCM3 simulations forced by the observed time-varying SST. The ensemble response to the El Niño SST displays a PNA-like pattern in both early and late winter. Therefore, the SST-forced circulation is unable to describe the differences between early and late winter circulation patterns. The EOF analysis on the individual CCM3 runs suggests that the internal variability of the atmosphere tends to decrease the frequency of occurrence of the PNA pattern in El Niño years. As mentioned

TABLE 4. Number of months with the PNA pattern in CCM3. The values in parentheses are the averages of EOF analyses of individual CCM3 runs.

Percentage of variance	45 yr (1950–94)	9 El Niño yr	Percentage of occurrence in the 9 El Niño yr
Nov 38% (Mode 1)	13 (14.7)	5 (4.3)	38% (29%)
Dec 41% (Mode 1)	13 (15.1)	6 (4.4)	46% (29%)
Jan 38% (Mode 1)	13 (15.8)	6 (4.8)	46% (30%)
Feb 48% (Mode 1)	16 (14.3)	8 (4.5)	50% (32%)
Mar 40% (Mode 1)	13 (13.4)	6 (3.8)	46% (28%)

earlier, there are some other mechanisms responsible for generating and maintaining the PNA pattern, including climatological mean flow and storm tracks (Simmons et al. 1983; Kok and Opsteegh 1985). The observed correlations between the PNA pattern and the North Pacific SST may be the manifestation of the interactions between the North Pacific SST and these atmospheric processes, including the internal atmospheric variability. Given a strong association of the PNA pattern with the North Pacific SST, the climate predictions based on ensemble model response to the tropical SST should be interpreted with caution.

Nonlinearity is another issue in the influence of tropical SST on the extratropical circulation. Hoerling et al. (1997) revealed the existence of nonlinear extratropical responses between El Niño and La Niña events. In addition to the polarity of the SST, the differences in atmospheric responses to weak and strong El Niño also reflect one aspect of the nonlinearity. Even in a single El Niño event, the magnitudes of the SST anomalies vary with time. It would be interesting to extend this study to the influences of both intensities and evolution of the El Niño SST on the extratropical circulation, and to the La Niña case as well.

Acknowledgments. This study was supported by the New Investigator Program (NIP) of the NASA EOS. We thank the NCAR Atmosphere Model Working Group, who conducted the CCM3 integrations, and Dr. Arun Kumar for access to the CCM3 output. We also thank Margaret Sanderson Rae and Cas Sprout for editorial assistance and two anonymous reviewers for their constructive comments and suggestions, which led to great improvements in the presentation of the results.

REFERENCES

- Alexander, M. A., 1990: Simulation of the response of the North Pacific Ocean to the anomalous atmospheric circulation associated with El Niño. *Climate Dyn.*, **5**, 53–65.
- , 1992: Midlatitude atmosphere–ocean interaction during El Niño. Part I: The North Pacific Ocean. *J. Climate*, **5**, 944–958.
- Barnston, A. G., and R. E. Livezey, 1987: Classification, seasonality and persistence of low-frequency atmospheric circulation patterns. *Mon. Wea. Rev.*, **115**, 1083–1126.
- Blackmon, M. L., J. E. Geisler, and E. J. Pitcher, 1983: A general circulation model study of January climate anomaly patterns

- associated with interannual variation of equatorial Pacific sea surface temperatures. *J. Atmos. Sci.*, **40**, 1410–1425.
- Bretherton, C. S., C. Smith, and J. M. Wallace, 1992: An intercomparison of methods for finding coupled patterns in climate data. *J. Climate*, **5**, 541–560.
- Halpert, M. S., and C. F. Ropelewski, 1992: Surface temperature patterns associated with the Southern Oscillation. *J. Climate*, **5**, 577–593.
- Held, I. M., S. W. Lyons, and S. Nigam, 1989: Transients and the extratropical response to El Niño. *J. Atmos. Sci.*, **46**, 163–174.
- Higgins, R. W., J. E. Janowiak, and Y. Yao, 1996: A gridded hourly precipitation data base for the United States (1963–1993). *NCEP/Climate Prediction Center ATLAS No. 1*, 46 pp.
- Hoerling, M. P., and M. Ting, 1994: Organization of extratropical transients during El Niño. *J. Climate*, **7**, 745–766.
- , A. Kumar, and M. Zhong, 1997: El Niño, La Niña, and the nonlinearity of their teleconnections. *J. Climate*, **10**, 1769–1786.
- Horel, J. D., and J. M. Wallace, 1981: Planetary scale atmospheric phenomena associated with the Southern Oscillation. *Mon. Wea. Rev.*, **109**, 813–829.
- Hoskins, B., and D. Karoly, 1981: The steady linear response of a spherical atmosphere to thermal and orographic forcing. *J. Atmos. Sci.*, **38**, 1179–1196.
- , A. J. Simmons, and D. G. Andrews, 1977: Energy dispersion in a barotropical atmosphere. *Quart. J. Roy. Meteor. Soc.*, **103**, 553–568.
- Kiehl, J. T., J. J. Hack, G. B. Bonan, B. A. Boville, D. L. Williamson, and P. J. Rasch, 1998: The National Center for Atmospheric Research Community Climate Model: CCM3. *J. Climate*, **11**, 1131–1149.
- Kok, C. J., and J. D. Opsteegh, 1985: On the possible causes of anomalies in seasonal mean circulation patterns during the 1982–83 El Niño event. *J. Atmos. Sci.*, **42**, 677–694.
- Lau, N.-C., 1985: Modeling the seasonal dependence of the atmospheric response to observed El Niño in 1962–76. *Mon. Wea. Rev.*, **113**, 1970–1996.
- , and M. J. Nath, 1996: The role of the “atmospheric bridge” in linking tropical Pacific ENSO events to extratropical SST anomalies. *J. Climate*, **9**, 2036–2057.
- Livezey, R. E., and K. C. Mo, 1987: Tropical–extratropical teleconnections during the Northern Hemisphere winter. Part II: Relationships between monthly mean Northern Hemisphere circulation patterns and proxies for tropical convection. *Mon. Wea. Rev.*, **115**, 3115–3132.
- , M. Masutani, A. Leetmaa, H. Rui, M. Ji, and A. Kumar, 1997: Teleconnective response of the Pacific–North American region atmosphere to large central equatorial Pacific SST anomalies. *J. Climate*, **10**, 1787–1820.
- Montroy, D. L., 1997: Linear relation of central and eastern North American precipitation to tropical Pacific sea surface temperature anomalies. *J. Climate*, **10**, 541–558.
- , M. B. Richman, and P. J. Lamb, 1998: Observed nonlinearities of monthly teleconnections between tropical Pacific sea surface temperature anomalies and central and eastern North American precipitation. *J. Climate*, **11**, 1812–1835.
- Newman, M., and P. D. Sardeshmukh, 1998: The impact of the annual cycle on the North Pacific/North American response to remote low-frequency forcing. *J. Atmos. Sci.*, **55**, 1336–1353.
- Ropelewski, C. F., and M. S. Halpert, 1986: North American precipitation and temperature patterns associated with the El Niño/Southern Oscillation (ENSO). *Mon. Wea. Rev.*, **114**, 2352–2362.
- , and —, 1987: Global and regional scale precipitation patterns associated with the El Niño/Southern Oscillation. *Mon. Wea. Rev.*, **115**, 1606–1626.
- Saravanan, R., 1998: Atmospheric low-frequency variability and its relationship to midlatitude SST variability: Studies using the NCAR Climate System Model. *J. Climate*, **11**, 1386–1404.
- Simmons, A. J., J. M. Wallace, and G. W. Branstator, 1983: Barotropic wave propagation and instability, and atmospheric teleconnection patterns. *J. Atmos. Sci.*, **40**, 1363–1392.
- Smith, T. M., R. W. Reynolds, R. E. Livezey, and D. C. Stokes, 1996: Reconstruction of historical sea surface temperature using empirical orthogonal functions. *J. Climate*, **9**, 1403–1420.
- Ting, M., and H. Wang, 1997: Summertime U.S. precipitation variability and its relation to Pacific sea surface temperature. *J. Climate*, **10**, 1853–1873.
- Trenberth, K. E., 1997: The definition of El Niño. *Bull. Amer. Meteor. Soc.*, **78**, 2771–2777.
- , G. W. Branstator, D. Karoly, A. Kumar, N.-C. Lau, and C. Ropelewski, 1998: Progress during TOGA in understanding and modeling global teleconnections associated with tropical sea surface temperatures. *J. Geophys. Res.*, **103**, 14 291–14 324.
- Vose, R. S., R. L. Schmoyer, P. M. Steurer, T. C. Peterson, R. Heim, T. R. Karl, and J. Eischeid, 1992: The global historical climatology network: Long-term monthly temperature, precipitation, sea level pressure, and station pressure data. Carbon Dioxide Information Analysis Center NDP-041, Oak Ridge National Laboratory, Oak Ridge, TN, 15 pp. [Available from CDIAC, Oak Ridge National Laboratory, P.O. Box 2008, Oak Ridge, TN 37831-6335.]
- Wallace, J. M., and D. Gutzler, 1981: Teleconnection in the geopotential height field during the Northern Hemisphere winter. *Mon. Wea. Rev.*, **109**, 784–812.
- , and Q.-R. Jiang, 1987: On the observed structure of the interannual variability of the atmosphere/ocean climate system. *Atmospheric and Oceanic Variability*, H. Cattle, Ed., Royal Meteorology Society, 17–43.
- , C. Smith, and C. S. Bretherton, 1992: Singular value decomposition of wintertime sea surface temperature and 500-mb height anomalies. *J. Climate*, **5**, 561–576.
- Wang, H., 1997: An observational and modeling study of the relationships between United States precipitation and Pacific sea surface temperature. Ph.D. thesis, University of Illinois, Urbana–Champaign, 136 pp. [Available from UMI No. 9812801, 300 North Zeeb Rd., Ann Arbor, MI 48106-1346.]
- Zhang, Y., J. M. Wallace, and N. Iwasaka, 1996: Is climate variability over the North Pacific a linear response to ENSO? *J. Climate*, **9**, 1469–1478.